RESEARCH ARTICLE

Enhanced Oral Absorption and Bioavailability of Ivermectin Through Amorphous Solid Dispersion Techniques

Chang Y*, Li J, Zou Z Z*

Department of DMPK&TOX, Global Health Drug Discovery Institute,Unit 2-B, Zhongguancun Dongsheng International Science Park, 1 North Yongtaizhuang Road, Beijing 100192, China

Received: 21st Jun 2024; Revised: 23rd Oct, 2024; Accepted: 14th Nov, 2024; Available Online: 25th Dec, 2024

ABSTRACT

The purpose of this study was to develop a high-loading amorphous solid dispersion (ASD) of ivermectin to significantly enhance its oral absorption and bioavailability. Using a solvent method, we formulated a novel ternary ASD with polyvinylpyrrolidone PVPK30 and Poloxamer 188 (P188) in a 1:0.5:1.5 ratio of drug to PVPK30 to P188. We characterized the physicochemical properties of five ASD formulations through in vitro dissolution tests. The selected formulation, SD3, was further assessed using X-ray powder diffraction, scanning electron microscopy, differential scanning calorimetry, and pharmacokinetic studies in rats. Notably, SD3 enhanced drug loading more than 30-fold compared to commercial tablets. SD3 exhibited significantly faster dissolution rates and maintained an amorphous state that remained stable after two months of storage at 4°C. Pharmacokinetic analysis at a 20 mg/kg oral dose in rats showed that SD3 achieved the highest maximum concentration (Cmax), plasma exposure (AUC), and oral bioavailability compared to the pure drug and commercial tablets. The assessment of the oral absorption rate constant (Ka) revealed an increased Ka and intestinal permeability through this ASD, elucidating the possible mechanism behind these improvements.

Keywords: Ivermectin; Amorphous solid dispersion; Dissolution; Bioavailability.

How to cite this article: Chang Y, Li J, Zou Z Z. Enhanced Oral Absorption and Bioavailability of Ivermectin Through Amorphous Solid Dispersion Techniques. International Journal of Drug Delivery Technology. 2024;14(4):2013-22 . doi: 10.25258/ijddt.14.4.10

Source of support: Nil.

Conflict of interest: None

INTRODUCTION

Ivermectin (IVM) is a broad-spectrum antiparasitic agent used to treat a wide range of parasites, including nematodes, insects, and acari, in both animals and humans[1, 2]. Recently, its activity spectrum has expanded, showing potential in human therapeutics. Researchers have discovered that IVM has antiviral effects against COVID-19, Dengue, and HIV-1[3-5]. A blind clinical trial demonstrated that IVM has concentration-dependent antiviral effects in COVID-19 patients, significantly reducing the SARS-CoV-2 viral load at high systemic plasma concentrations[6, 7]. Additionally, Xinyi Tan found that IVM and an IVM-derived compound, D4, exhibit antimicrobial and biofilm properties against methicillin-resistant Staphylococcus aureus (MRSA)[8]. Furthermore, IVM shows potential as an anti-cancer drug by regulating multiple signaling pathways to inhibit tumor cell proliferation[9]. IVM is considered one of the most significant drugs ever discovered, with Satoshi Ōmura and William C. Campbell winning the 2015 Nobel Prize in Physiology or Medicine for its discovery[10].

However, Ivermectin is categorized as a Class II drug under the Biopharmaceutical Classification System, characterized by high permeability but low water solubility, leading to poor bioavailability when administered orally [11]. Various formulations have been developed to enhance its solubility and absorption, including solid dispersions [12-14], nanosuspensions [15], microemulsions [16], nanoparticles [17], polymer micelles [18], soluble cyclodextrin complexes [19], and self-emulsifying drug delivery systems [20]. Notable advancements include Marchenko's solid dispersion with arabinogalactan and Singh's surface solid dispersion with aerosil, both significantly improving water solubility and drug release rates. However, these methods often suffer from low drug loading capacities.

This study aims to develop a solid dispersion with a simple preparation process and high drug loading. Given IVM's high solubility in methanol and its high melting point, the solvent method was chosen to prepare the solid dispersion[21]. In our research, we selected two carriers based on a phase solubility study to develop a novel amorphous solid dispersion (IVM: carriers 1:2) using a solvent method aimed at improving the solubility, bioavailability, and drug loading of IVM. The physical properties of these IVM-SD formulations were assessed using X-ray diffraction analysis, scanning electron microscopy, differential scanning calorimetry, and dissolution tests. Our measurements indicate that the new solid dispersion not only improves solubility but also enhances bioavailability and increases the absorption rate constant (Ka) and intestinal permeability in Sprague-Dawley rat pharmacokinetics.

MATERIALS AND METHODS

Materials

The materials used in this study were IVM (MedChem Express (MCE) company), carriers like, PEG4000 (Alfa Aesar), PEG6000 (Alfa Aesar), D-Sorbitol (Innochem), Poloxamer188(P188, Rhawn), Urea (Sigma-Aldrich), Polyvinylpyrrolidone K30(PVPK30, Tci). Simulated

*Author for Correspondence: yu.chang@ghddi.org, zhiyang.zou@ghddi.org

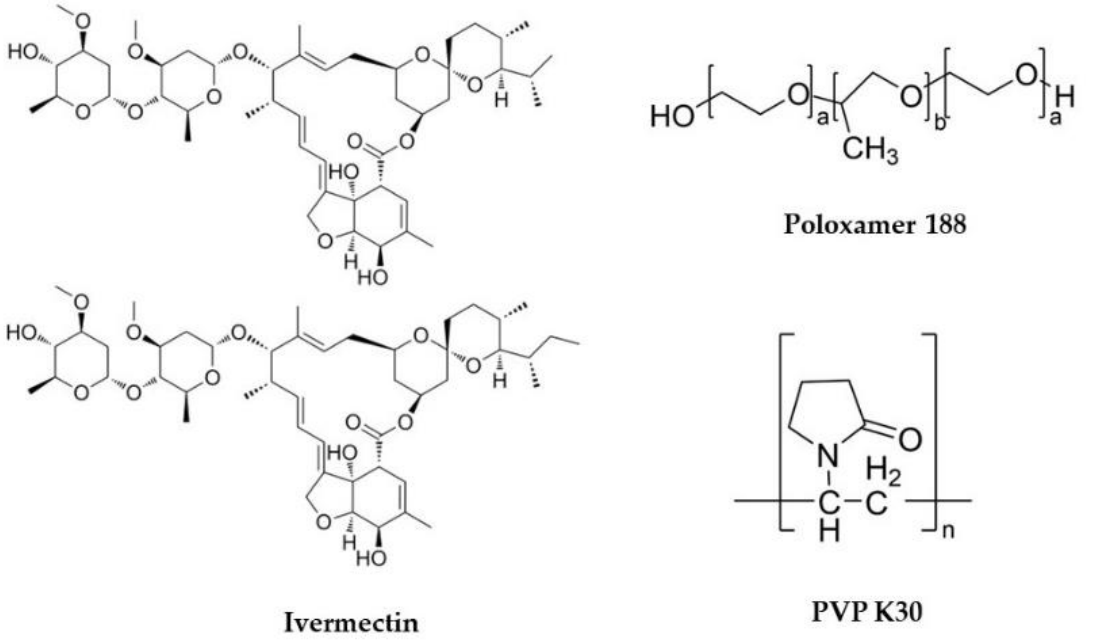

Figure 1: The chemical structure of IVM, PVPK30 and Poloxamer188.

intestine fluid was purchased from MesGenBiotech, and bile salt was purchased from Macklin. The commercial IVM tablet A was purchased from Nanhua Qianmu biological technology Co., LTD (Henan, China), which has ap-proximately 0.84% IVM. The commercial IVM tablet B was purchased from ShanXi Tianchong biological technology Co., LTD, which has approximately 0.96% IVM. The chemical structure of IVM, PVPK30 and Poloxamer188 were shown in Figure1.

Animals

Twelve male Sprague-Dawley rats, aging 6-8 weeks and weighting approximately 200-300 g, were used for pharmacokinetic study. The animal study protocol was approved by the Institutional Animal Care and Use Committee (IACUC) (protocol code PK-R-06012024 and date of approval: 24 April 2024).

Phase Solubility Study

To select suitable carriers for SD, the solubility of IVM in different carriers like PVPK30, P 188, D-sorbitol, PEG6000, PEG4000, Urea was investigated. Excess IVM was added to 1 ml containing 1% aqueous solution of carriers in glass vials, followed by stirring at 300 rpm for 24 h. Next, the contents were centrifuged at 10,000 rpm for 10 min by Eppendorf 5424R Centrifuge (Hamburg, Germany). Then the same volume of methanol was added to the supernatant. The amount of dissolved drug was estimated at 245 nm by UPLC-UV (Waters acquity UPLC and photodiode array (PDA) detector) using an acquity UPLC BEH C18 column (2.1× 50 mm, 1.7 µm).

Preparation of Solid Dispersion

IVM-SD were prepared by the solvent method. The weight ratio of drug and carriers (PVP K30 and P188) is 1:2. IVM and carriers were dissolved in methanol and vortexed for 10 min to obtain a clear solution. Subsequently, the solution was transferred to rotary evaporator (Buchi Vacuum pump V-300 and rotavapor R-300) and vacuum dried at 37°C, 150 rpm. Then the solid was transferred to ceramic mortar and milled to obtain the powder. All the powders were passed through sieve # 60. Carriers were mixed with IVM at varying ratios. In the procedure of SD preparation, we found that with a high percentage of P188, the SD showed sticky and inhomogeneous state. So, considering the state and dissolved quantity of SD formulation, we made a dissolution test to determine the optimal ratio of PVPK30 and P188. SD powders containing 5mg IVM were added to 100ml simulated intestine fluid with 0.2% bile salt monitored for 45min at 37°C, with 100 rpm of stirring. The dissolution experiment is more physiologically meaningful with adding 0.2% bile salt, because the bile salt appears in the gastrointestinal tract in physiological conditions[22, 23]. 200 ul samples were removed after 5, 10, 20, 30, 45 min for centrifugation at 10,000 rpm for 3 min. Each sample was tested in triplicate. Then the same volume of methanol was added to the supernatant. The removed sample was swapped for a commensurable amount of fresh dissolution medium to maintain the same volume in the vessel. The amount of dissolved drug was estimated at 245 nm by UPLC-UV.

Characterization of IVM-SD3

X-ray Powder Diffraction (XRD)

The drug crystallinity of IVM, PVPK30, P188 and SD3 formulations were measured using an automated X-ray diffractometer (D/max-2550, Japan). Data was collected over an angular range between 3° and 50° with a step size of 0.02. XRD patterns of SD3 stored in at 4 ◦C refrigerator for two months was also determined.

Differential Scanning Calorimetry (DSC)

The DSC thermograms of the samples were recorded using a differential scanning calorimeter instrument (Q5000IR, TA INSTRUMENTS, China). The 30mg samples were placed in aluminum pans and heated at a constant rate of 10◦C/min, over a temperature range of 0–300 ◦C. The flow of Nitrogen was 50 ml/min, which was used as purge gas.

Scanning Electron Microscopy (SEM)

The particle morphology of drug, PVPK30, P188 and SD3 were examined by scanning electron microscopy (SEM, JSM-6460LV, JEOL, Ltd, Japan). All the powders were passed through sieve # 60.

***In Vitro* Dissolution Study**

In dissolution profiles of IVM, physical mixtures, commercial tablets and SD3 were prepared. The powders containing 5 mg IVM were added to 100 ml simulated intestine fluid with 0.2% bile salt monitored for 45 min at 37°C, with 100 rpm of stirring. All powders were passed

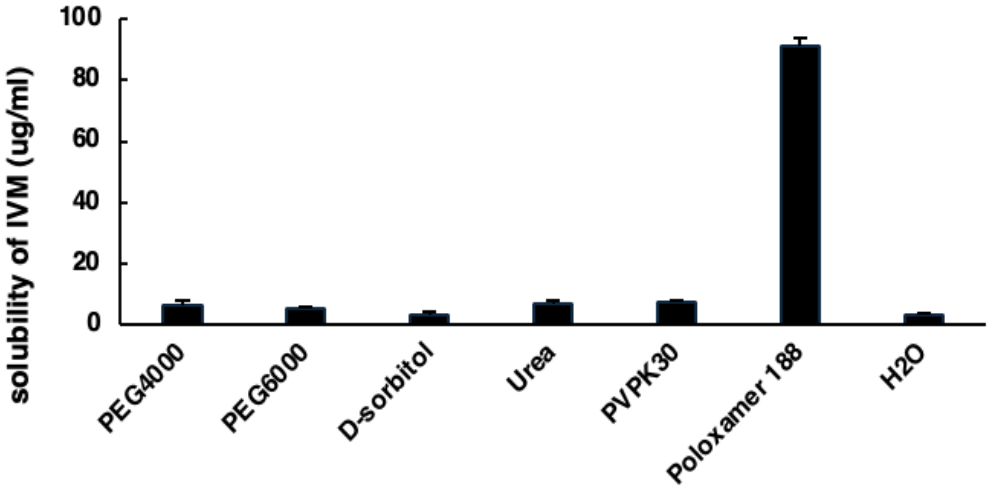

Figure 2: Influence of carriers on the solubility of IVM.

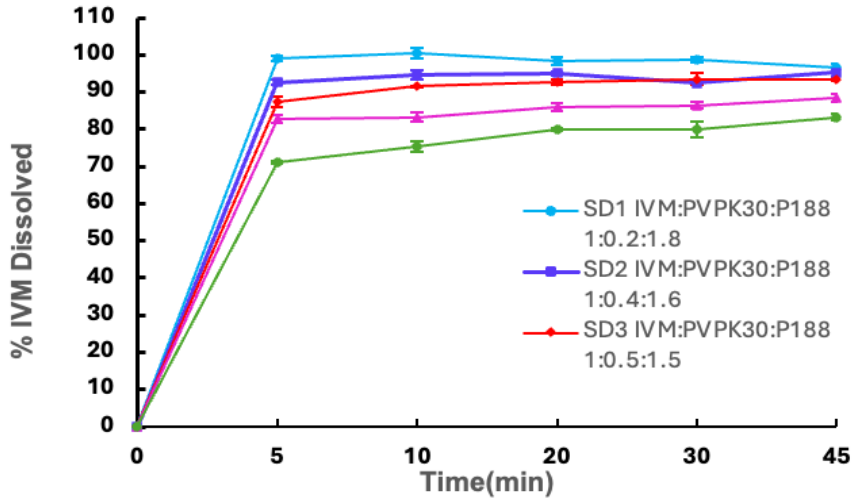

Figure 3: The dissolved quantity test of IVM-SD.

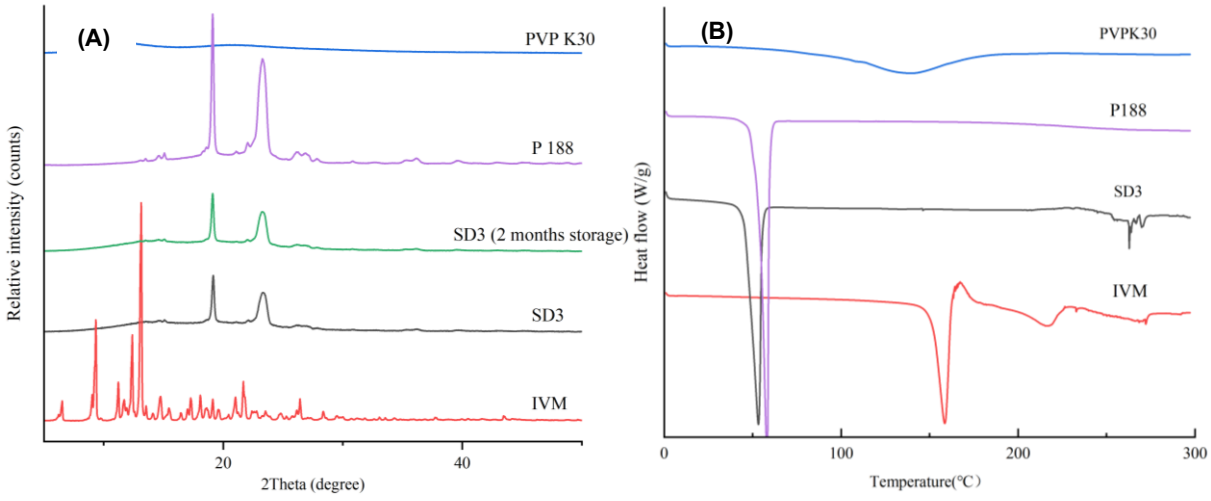

Figure 4(A): The X-ray powder diffraction patterns and (B) the differential scanning calorimetry thermograms of PVPK30, P188, SD3 and IVM.

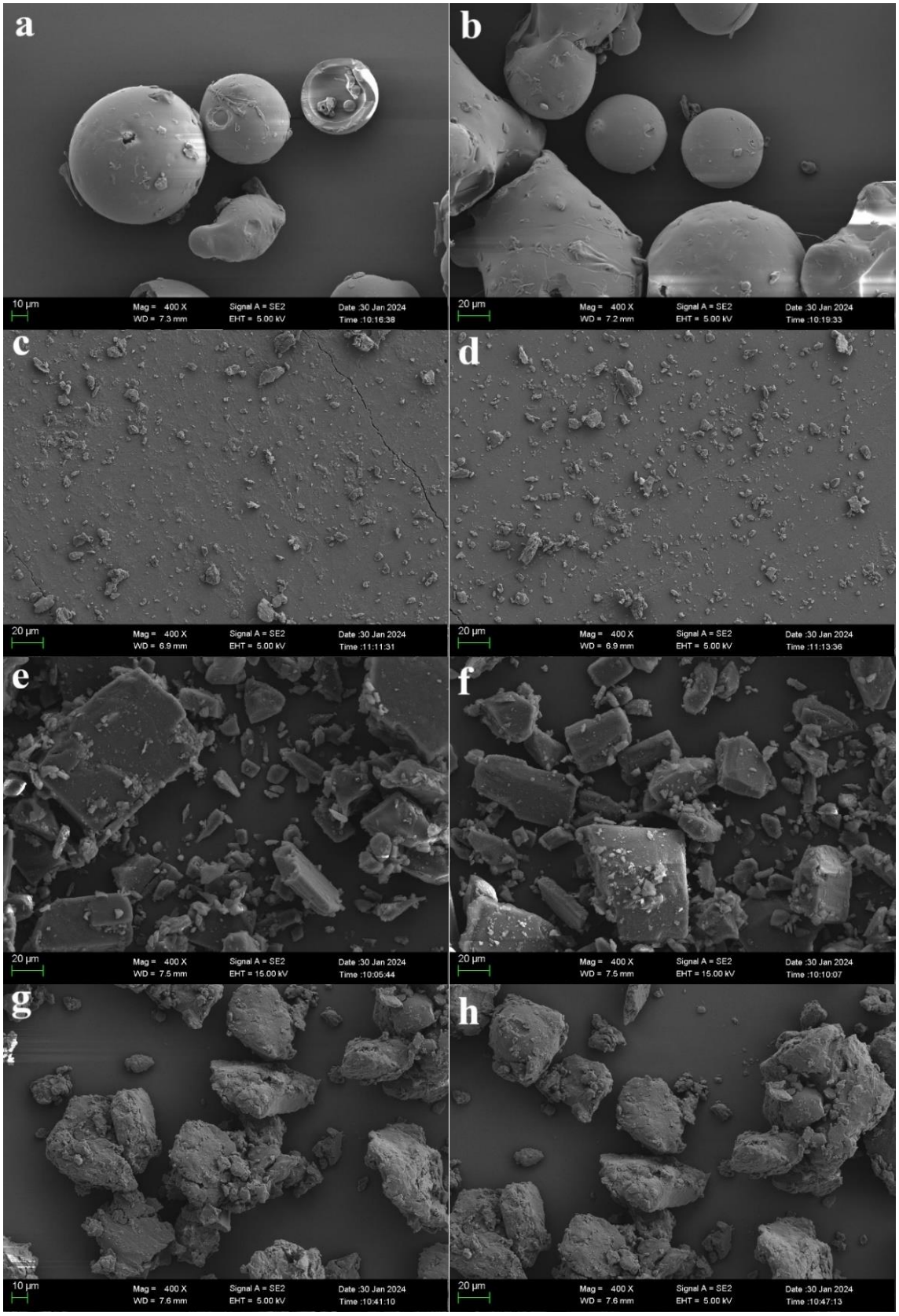

Figure 5**:** Scanning electron microphotographs. (a) PVPK30 400x, (b) PVPK30 400x, (c) P188 400x, (d) P188 400x, (e) IVM 400x, (f) IVM 400x, (g) solid dispersion 400x (SD3, IVM: PVPK30: P188=1:0.5:1.5), (h) solid dispersion 400x (SD3, IVM: PVPK30: P188=1:0.5:1.5).

through sieve # 60. Then 200 uL samples were removed after 5, 10, 20, 30, 45 min for centrifugation at 10,000 rpm for 3 min. Each sample was tested in triplicate. Then the same volume of methanol was added to the supernatant. The re-moved sample was replaced with an equivalent amount

of fresh dissolution medium to maintain a constant volume in the vessel. The amount of dissolved drug was estimated at 245 nm by UPLC-UV.

***In Vivo* Pharmacokinetic studies**

Animal Experiment

To evaluate the oral bioavailability of IVM-SD, four groups of Sprague Dawley rats (3 rats per group) were administered doses of equivalent 20 mg/kg IVM. Twelve male rats were fed with the pure drug, SD3, commercial tablet A, and commercial tablet B. Approximately 0.2 mL blood were collected at the time points for 0.25, 0.5, 1, 2, 4, 8, and 24 hours post dose and then were centrifugated at 4000 g for 5 minutes in a 4°C centrifuge. The plasma samples were stored in a freezer at -75±15°C prior to analysis.

LC-MS/MS Analysis of IVM

The LC-MS/MS method utilized an AB Sciex Triple Quad 5500 LC-MS/MS system with a column (Raptor Biphenyl 1.8 µm 30×2.1mm) to analyze the concentrations of IVM. 200 µL of acetonitrile containing IS mixture (IS: dexamethasone and verapamil) was added to 50 µL of rat plasma for precipitating protein. Then the samples were vortexed for 30 s. After centrifugation at 4°C, 4000 rpm for 15 min. 10 µL of diluted supernatant was injected into the LC/MS/MS system for quantitative analysis. The mobile phase for this study was 10 mM ammonium acetate solution in water (0.1%FA) (solvent A): 95% Acetonitrile in Water (0.1% Formic acid) (solvent B) with the flowing rate at 0.6 mL/min. The gradient was 0.20min, 80% solvent A: 20% solvent B; 0.80min, 0% solvent A: 100% solvent B;1.60min, 0% solvent A: 100% solvent B; 1.61min, 80% solvent A: 20% solvent B; 1.80min, 80% solvent A: 20% solvent B. The multiple reaction monitoring (MRM) of 892.39→569.10 m/z was used for IVM in plasma. A standard curve for IVM (1–1000 ng/mL) was prepared by serially diluting IVM stock solution. The intra-day and inter-day precision and accuracy variations were within 20%.

Data Analysis

WinNonlin (PhoenixTM, version 8.3) software was used for pharmacokinetic calculations. The pharmacokinetic

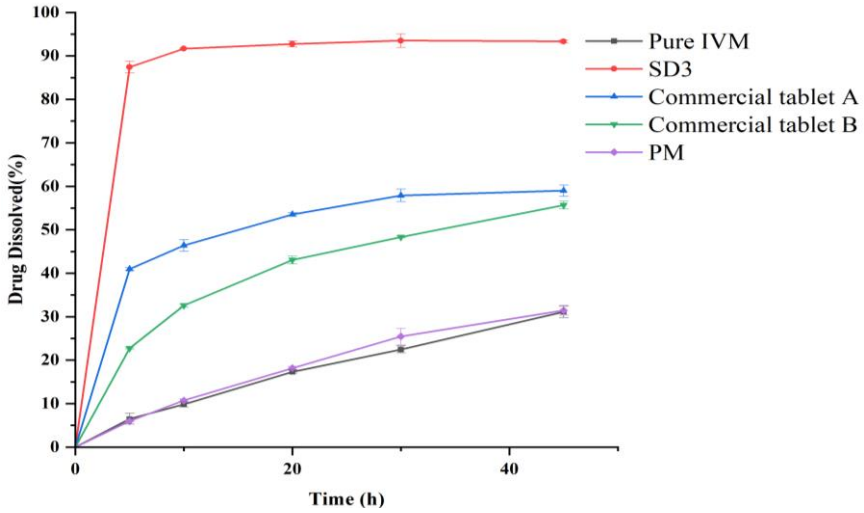

Figure 6: In vitro dissolution test of IVM, solid dispersion (SD3, IVM: PVPK30: P188=1:0.5:1.5), PM and commercial tablets.

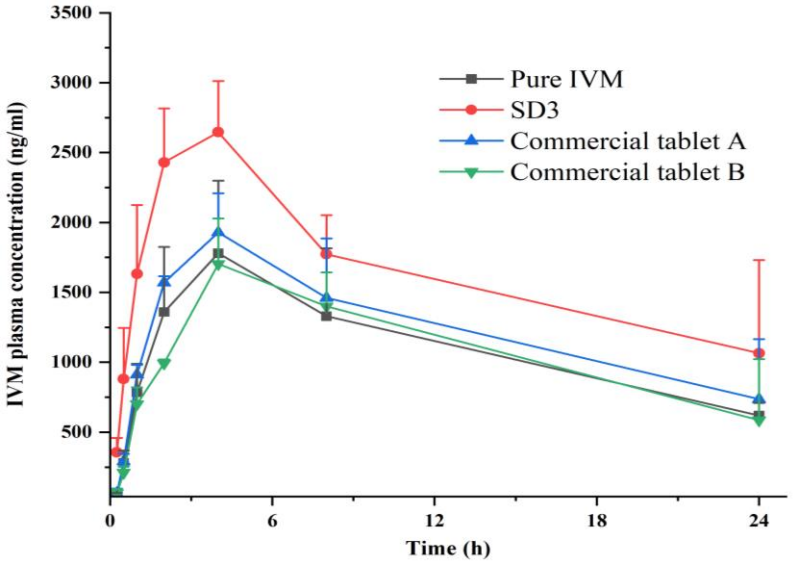

Figure 7. The mean concentration of IVM in rats' plasma after oral administration of pure IVM, SD3 and commercial tablets in a dosage of 20mg/kg (n=3).

Table 1. Pharmacokinetics parameters after administering pure IVM, SD3, commercial tablets to rats.

Parameters	Pure IVM	SD3	Commercial tablet A	Commercial tablet B
$T_{1/2}$ (h)	16.0±8.1	21.6±18.4	16.4±4.7	14.6±10
T_{max} (h)	4.00±0.00	3.33±1.15	3.33±1.15	4.00±0.00
C_{max} (ng/mL)	1780±520	2657±369	1930±280	1703±325
AUC_{last} (h*ng/mL)	26342±6844	39479±9434	22822±10939	25900±6350
AUC_{Inf} (h*ng/mL)	41137±5488	84336±67839	50121±19279	42435±27305
MRT_{Inf}_obs (h)	24.1±12.8	31.8±27.2	24.7±7.4	21.8±15.1
Cl/F_obs (mL/h/kg)	492±70.8	339±193	455±218	590±277

$T_{1/2}$, elimination half-life; T_{max}: time to reach C_{max}; C_{max}, maximum plasma concentration; AUC_{last}, area under the plasma concentration curve from zero to 24 h; AUCinf, area under the plasma concentration curve from zero to infinity; MRT, mean residence time; Cl/F_obs, the parent clearance.

data will be described using descriptive statistics such as mean, standard deviation.

Absorption rate constant (Ka) calculation

A method of residuals was used to calculate Ka. Starting with the equation (1) for Cp versus time after oral administration:

Cp=F*Dose*Ka*[e-Kel*t-e-Ka*t]/V*(Ka-Kel)…(1)

Where, A= F*Dose*Ka/V*(Ka-Kel)

Equation (1) can be written as:

Cp=A*e-Kel*t-A*e-Ka*t …(2)

Where, C_{plate}=A*e-Kel*t

Plotting Cplate versus time gives a straight line on semi-log graph paper, with a slope (ln) = -kel and intercept = A.

Equation (2) can be written as:

Cplast-Cp= A*e-Ka*t…(3)

Where, Residual=Cplast-Cp

Plotting the ln (Residual) versus time should give another straight-line graph with a slope (ln) equal to - ka and the intercept as before, i.e. A.

Cp is plasma concentration at time t, F is bioavailability, V is volume distribution and Kel is elimination rate constant.

RESULTS AND DISCUSSION

Phase Solubility Study

The effects of different carriers on the solubility of IVM were shown in Figure 2. Among the carriers, P 188 showed the highest solubility, which can increase the solubility of IVM to 91.28ug/ml. The results indicated a strong affinity between IVM and the co-polymer P188, which is beneficial for enhancing IVM's solubility in water. As depicted in Figure 1, an ivermectin molecule comprises three hydroxyl groups, whereas P188 features numerous oxygen atoms serving as hydrogen bond acceptors. Additionally, both ivermectin and P188 contain several ether units. According to the "Like Dissolves Like" principle, this structural similarity contributes to their strong affinity for each other[24, 25]. However, in our research, P188 as a carrier, SD was so sticky and hard to operate. In addition, binary systems have some big challenges such as physical stability, wettability,

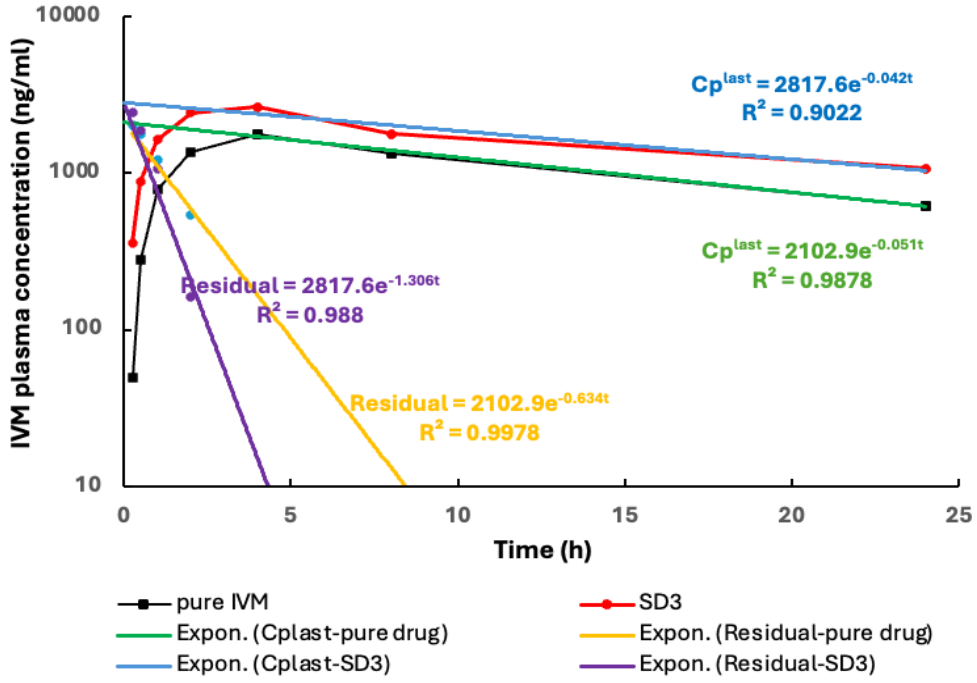

Figure 8: The Ka calculation of pure IVM and SD3 after oral administration in a dosage of 20mg/kg.

precipitation in dissolution media, and processability[26]. Review of research findings, ternary solid dispersion systems can solve these difficulties by incorporating a third component into the formulation[27, 28]. So, we chose combined carriers to make the solid dispersion. Through phase solubility study, we found that PVP K30 also can increase the solubility of IVM to 7.52 ug/ml. And PVPK30 is a hydrophilic polymer and the most used in SD formulations[29]. Therefore, we chose PVPK30 and P188 to make the SD of IVM, and because the hydrotropy of P188 was stronger than PVPK30, the ratio of P188 was higher.

Optimization of the ratio of PVPK30 and P188

The results were shown in Figure 3. The dissolved quantity of all SDs was above 80%. We also found that with the increasing proportion of P188, SD had the higher dissolved quantity, this result was consistent with the phase solubility. However, in the SD preparation, a high percentage of P188 made the inhomogeneous state. Taking overall consideration of all the factors involved, SD3 is the best. We chose SD3 for further evaluation.

Characterization of IVM-SD3

XRD Analysis

XRD is a widely used method to investigate the state of the pure drug and its polymer blend, which was amorphous or crystalline[30, 31]. The XRD results of IVM, PVPK30, P188 and SD3 were shown in Figure 4(A). The diffraction pattern of PVPK30 showed no sharp peaks, indicating this polymer was amorphous state. The diffraction spectra of IVM pure drug had high and sharp peaks (red line) at diffraction angle from 6.54° to 26.45°. The sharp peaks mean the presence of a crystalline form of the drug. SD3 showed only diffraction peaks at 19.14° and 23.21°, while P 188 also had peaks at the same diffraction angle, which indicated the peaks in SD3 were the crystals of P188. In conclusion, SD3 showed an amorphous state. It may be due to the inhibition of crystallization of PVPK30, may through a possible chemical interaction (such as hydrogen bonding between the drug molecules and the polymer), the other reason may be the process of solvent evaporation used for preparing solid dispersions[32, 33]. After the SD3 were kept in 4°C for 2 months, there were no changes in XRD pattern, which indicated SD3 were stable during storage.

DSC Analysis

The differential scanning calorimetric of the IVM, PVPK30, P188 and SD3 formulations are shown in Fig.4B. The DSC thermogram of PVPK30 showed a small endothermic peak at 138°C, and P188 showed an endothermic peak at 56°C, corresponding to melting point respectively. IVM had an endothermic peak at 158°C, corresponding to its melting point. SD3 displayed changes in the peak, where it shifted to a very low melting temperature of 51.9°C. This phenomenon may be due to the mixing effect of amorphous IVM and carriers[34]. In Figure 4(B), we cannot find the endothermic peak of IVM in SD3, which indicated the disappearance of crystalline of pure drug[35, 36]. The results of XRD and DSC were consistent, indicating that SD3 was in an amorphous state.

SEM Analysis

The scanning electron micrographs of the IVM, PVPK30, P188 and SD3 formulations were shown in Fig.5. The IVM powder (Figure 5e, f) had irregular crystals, which were different shapes and sizes. PVPK30 (Figure 5a, b) and P188 (Figure 5c, d) showed typical morphologies. SD3 (Figure 5g, h) had fuzzy contours, suggesting that the drug appeared to be amorphous and attached to the surface of hydrophilic polymer and surfactant.

***In Vitro* Dissolution Study**

The results of the dissolution tests for IVM, physical mixture (PM), commercial tablets and SD3 over the period of 45 min were shown to Figure 6. PM was prepared at the same ratio of IVM: PVPK30: P188=1:0.5:1.5 as SD3, also was milled and sieved (sieve # 60). From Figure 6, pure IVM had low dissolution. We also found that the dissolution was not changed by only adding carriers to IVM (physical mixture), which indicated that amorphous status plays a role in dissolution. At 45min, SD3 showed the highest percentage of drug release, indicating the formulation of combined carriers PVPK30 and P188 with solvent method can be a good strategy to improve the drug release and solubility of IVM. Compared with the about 50% dissolution percentage of commercial tablets, SD3 could reach 93% at the same conditions. Also, for an initial 5 min, the dissolved percentage of SD3 increased faster to 87%, indicating solid dispersion had the faster drug release rate. This result may be related to the physical-chemical properties of P188 and PVPK30. P188 had better solubility and wettability[37, 38], and PVPK30 inhibited the crystallization of drug, resulting in the amorphous state form of IVM[39]. Also, the amorphous state of IVM in SD3, which can help increase dissolution rate, because no energy is required to break up the crystal lattice[40]. Then the results of in vitro dissolution tests were validated using oral pharmacokinetics of SD3 in Sprague Dawley rats.

***In Vivo* Pharmacokinetic studies**

In this pharmacokinetic study, we used SD3, the pure drug and commercial tablets to verify the correlation between the in vivo and in vitro performance. The mean plasma concentration-time profiles and pharmacokinetic parameters of IVM (Cmax, T1/2, Tmax, AUClast, AUCinf, MRTinf and Cl/F) obtained after oral administration were shown in Figure 7 and Table I. The correlation coefficient of calibration curve of the IVM in plasma was 0.9972. The results showed that the plasma exposure of IVM in SD3 increased compared with the pure drug and commercial tablets. The bioavailability of commercial tablet B was slightly worse than pure drug. The AUClast were 26342 h*ng/mL, 39479 h*ng/mL, 22822 h*ng/mL and AUCinf were about 41137 h*ng/mL, 84336 h*ng/mL, 50121 h*ng/mL for pure drug, SD3 and commercial tablet A respectively. The relative oral bioavailability of SD3 and commercial tablet A were 205%, 122% compared to pure drug. The maximum peak plasma concentration (Cmax) of pure drug, SD3 and commercial tablets were 1780 ng/mL, 2657 ng/mL, 1930 ng/mL and 1703 ng/mL respectively. SD3 enhanced the Cmax of the drug, accounting for 1.49 (pure drug), 1.38 (commercial tablet A) and 1.56-fold (commercial tablet B) improvement. Compared to pure drug, the clearance of the drug in SD3 was reduced from 492 mL/h/kg to 339 mL/h/kg, resulting in the increased T1/2 from 16.0 h to 21.6h. Compared to commercial tablets,

though SD3 showed 39.6 and 34.7 -fold improvement of drug loading, the clearance of the drug in SD3 was reduced from 455 mL/h/kg(commercial tablet A) and 590 mL/h/kg(commercial tablet B) to 339 mL/h/kg, resulting in the increased T1/2 from 16.4 h (commercial tablet A) and 14.6h (commercial tablet B) to 21.6h. Thus, the solid dispersion of IVM with PVPK30 and P188 in a 1:0.5:1.5 ratio improved solubility and dissolution, which was translated in higher rat PK oral bioavailability.

Absorption rate constant (Ka) calculation and intestinal permeability

The results for the absorption rate constant (Ka) of the pure drug and the solid dispersion SD3 are shown in Figure 8. We found that the Ka values for the pure drug and SD3 were 0.634 h^{-1} and 1.306 h^{-1}, respectively, indicating that the Ka of SD3 was 2.05 times higher than that of the pure drug. This increased rate not only raises the maximum plasma concentration (Cmax) but also reduces the time to reach Cmax (Tmax) [41, 42]. P188, a nonionic surfactant, effectively inhibits P-glycoprotein (P-gp) transport, thereby increasing the intestinal permeability of IVM [43]. Additionally, IVM itself acts as both an inhibitor and a substrate of P-gp transport, with an inhibition IC50 of 440 nM [44]. In our amorphous solid dispersion SD3, the concentration of IVM is significantly higher than that of pure IVM, which provides greater inhibition and saturation of P-gp efflux in the intestine. This leads to an increased Ka and enhances intestinal permeability[45, 46].

CONCLUSION

In this study, we have engineered a robust IVM amorphous solid dispersion (SD3) through meticulous optimization of carrier ratios. XRD, DSC and SEM analysis indicated that IVM showed the amorphous state in solid dispersion. This advancement streamlines production processes, augments drug loading, and notably improves absorption and bioavailability, including the absorption constant Ka and intestinal permeability. Our innovative formulation surpasses commercial tablets, yielding elevated plasma exposure. Consequently, it emerges as a promising therapeutic option, potentially enhancing clinical efficacy.

Acknowledgments

This work was supported in whole by the Bill & Melinda Gates Foundation Grant Number [INV-008249]. Under the grant conditions of the Foundation, a Creative Commons Attribution 4.0 Generic License has already been assigned to the Author Accepted Manuscript version that might arise from this submission.

REFERENCES

1. Dourmishev AL, Dourmishev LA and Schwartz RA. Ivermectin: pharmacology and application in dermatology. *Int J Dermatol* 2005; 44: 981-988. 2006/01/18. DOI: 10.1111/j.1365-4632.2004.02253.x.
2. Ashour DS. Ivermectin: From theory to clinical application. *Int J Antimicrob Agents* 2019; 54: 134-142. 2019/05/10. DOI: 10.1016/j.ijantimicag.2019.05.003.
3. Caly L, Druce JD, Catton MG, et al. The FDA-approved drug ivermectin inhibits the replication of SARS-CoV-2 in vitro. *Antiviral Res* 2020; 178: 104787. 2020/04/07. DOI: 10.1016/j.antiviral.2020.104787.
4. Ooi EE. Repurposing ivermectin as an anti-dengue drug. Oxford University Press US, 2021, p. e594-e595.
5. Wagstaff KM, Sivakumaran H, Heaton SM, et al. Ivermectin is a specific inhibitor of importin α/β-mediated nuclear import able to inhibit replication of HIV-1 and dengue virus. *Biochemical Journal* 2012; 443: 851-856.
6. Krolewiecki A, Lifschitz A, Moragas M, et al. Corrigendum to Antiviral effect of high-dose ivermectin in adults with COVID-19: A proof-of-concept randomized trial [EClinicalMedicine 37 (2021) 100,959]". *EClinicalMedicine* 2021; 39: 101119. 2021/09/01. DOI: 10.1016/j.eclinm.2021.101119.
7. Krolewiecki A, Lifschitz A, Moragas M, et al. Antiviral effect of high-dose ivermectin in adults with COVID-19: A proof-of-concept randomized trial. *EClinicalMedicine* 2021; 37: 100959. 2021/07/01. DOI: 10.1016/j.eclinm.2021.100959.
8. Tan X, Xie H, Zhang B, et al. A Novel Ivermectin-Derived Compound D4 and Its Antimicrobial/Biofilm Properties against MRSA. *Antibiotics (Basel)* 2021; 10 2021/03/07. DOI: 10.3390/antibiotics10020208.
9. Tang M, Hu X, Wang Y, et al. Ivermectin, a potential anticancer drug derived from an antiparasitic drug. *Pharmacol Res* 2021; 163: 105207. 2020/09/25. DOI: 10.1016/j.phrs.2020.105207.
10. Crump A. Ivermectin: enigmatic multifaceted 'wonder' drug continues to surprise and exceed expectations. *J Antibiot (Tokyo)* 2017; 70: 495-505. 2017/02/16. DOI: 10.1038/ja.2017.11.
11. Lindenberg M, Kopp S and Dressman JB. Classification of orally administered drugs on the World Health Organization Model list of Essential Medicines according to the biopharmaceutics classification system. *Eur J Pharm Biopharm* 2004; 58: 265-278. 2004/08/07. DOI: 10.1016/j.ejpb.2004.03.001.
12. Marchenko VA, Khalikov SS, Efremova EA, et al. Efficacy of Novel Formulations of Ivermectin and Albendazole in Parasitic Infections of Sheep in the Altai Mountains of Russia. *Iran J Parasitol* 2021; 16: 199-208. 2021/09/25. DOI: 10.18502/ijpa.v16i2.6268.
13. Singh D and Pathak K. Hydrogen bond replacement--unearthing a novel molecular mechanism of surface solid dispersion for enhanced solubility of a drug for veterinary use. *Int J Pharm* 2013; 441: 99-110. 2012/12/25. DOI: 10.1016/j.ijpharm.2012.12.008.
14. Verma S, Patel U and Patel RP. Formulation and evaluation of ivermectin solid dispersion. *Journal of Drug Delivery and Therapeutics* 2017; 7: 15-17.
15. Starkloff WJ, Bucala V, Palma SD, et al. Design and in vitro characterization of ivermectin nanocrystals liquid formulation based on a top-down approach. *Pharm Dev Technol* 2017; 22: 809-817. 2016/06/28. DOI: 10.1080/10837450.2016.1200078.
16. Das S, Lee SH, Chia VD, et al. Development of microemulsion based topical ivermectin formulations: Pre-formulation and formulation studies. *Colloids Surf*

B Biointerfaces 2020; 189: 110823. 2020/02/10. DOI: 10.1016/j.colsurfb.2020.110823.
17. Guo D, Dou D, Li X, et al. Ivermection-loaded solid lipid nanoparticles: preparation, characterisation, stability and transdermal behaviour. *Artif Cells Nanomed Biotechnol* 2018; 46: 255-262. 2017/04/04. DOI: 10.1080/21691401.2017.1307207.
18. Dong J, Song X, Lian X, et al. Subcutaneously injected ivermectin-loaded mixed micelles: formulation, pharmacokinetics and local irritation study. *Drug Deliv* 2016; 23: 2220-2227. 2016/10/18. DOI: 10.3109/10717544.2014.956849.
19. Mansour SM, Shamma RN, Ahmed KA, et al. Safety of inhaled ivermectin as a repurposed direct drug for treatment of COVID-19: A preclinical tolerance study. *International Immunopharmacology* 2021; 99: 108004.
20. Patel VP, Lakkad HA and Ashara KC. Formulation Studies of Solid Self-Emulsifying Drug Delivery System of Ivermectin. *Folia Med (Plovdiv)* 2018; 60: 580-593. 2019/06/13. DOI: 10.2478/folmed-2018-0024.
21. Rolim LA, dos Santos FCM, Chaves LL, et al. Preformulation study of ivermectin raw material. *Journal of Thermal Analysis and Calorimetry* 2015; 120: 807-816.
22. Damian F, Blaton N, Naesens L, et al. Physicochemical characterization of solid dispersions of the antiviral agent UC-781 with polyethylene glycol 6000 and Gelucire 44/14. *Eur J Pharm Sci* 2000; 10: 311-322. 2000/06/06. DOI: 10.1016/s0928-0987(00)00084-1.
23. de Oliveira Eloy J, Saraiva J, de Albuquerque S, et al. Solid dispersion of ursolic acid in Gelucire 50/13: a strategy to enhance drug release and trypanocidal activity. *AAPS PharmSciTech* 2012; 13: 1436-1445. 2012/10/17. DOI: 10.1208/s12249-012-9868-2.
24. Smith WL. Selective solubility:" Like dissolves like". *Journal of Chemical Education* 1977; 54: 228.
25. Zhuang B, Ramanauskaite G, Koa ZY, et al. Like dissolves like: A first-principles theory for predicting liquid miscibility and mixture dielectric constant. *Sci Adv* 2021; 7 2021/02/14. DOI: 10.1126/sciadv.abe7275.
26. Newman A, Engers D, Bates S, et al. Characterization of amorphous API:Polymer mixtures using X-ray powder diffraction. *J Pharm Sci* 2008; 97: 4840-4856. 2008/03/21. DOI: 10.1002/jps.21352.
27. Budiman A, Lailasari E, Nurani NV, et al. Ternary Solid Dispersions: A Review of the Preparation, Characterization, Mechanism of Drug Release, and Physical Stability. *Pharmaceutics* 2023; 15 2023/08/26. DOI: 10.3390/pharmaceutics15082116.
28. Jafar M, Salahuddin M, Kayed M, et al. Solid state analysis and in-vitro dissolution behavior of meloxicam-hydroxy propyl beta cyclodextrin-ethanolamines ternary complexes. *International Journal of Pharmaceutical Quality Assurance* 2018; 9: 298-304. DOI: 10.25258/ijpqa.v9i01.11919.
29. Wagh VT, Gilhotra RM and Wagh RD. Solid dispersion (Kneading) technique: a platform for enhancement dissolution rate of valsartan poorly water-soluble drug. *International Journal of Pharmaceutical Quality Assurance* 2020; 11: 20-24.
30. Fo'ad T, Hameed GS and Raauf AM. Thermal Analysis in the Pre-formulation of Amorphous Solid Dispersion for Poorly Water-soluble Drugs. *International Journal of Drug Delivery Technology* 2022; 12: 1595-1599. DOI: 10.25258/ijddt.12.4.19.
31. Anjana R, Kumar S, Sharma H, et al. Phytosome drug delivery of natural products: A promising technique for enhancing bioavailability. *International Journal of Drug Delivery Technology* 2017; 7: 157-165.
32. Frizon F, de Oliveira Eloy J, Donaduzzi CM, et al. Dissolution rate enhancement of loratadine in polyvinylpyrrolidone K-30 solid dispersions by solvent methods. *Powder technology* 2013; 235: 532-539.
33. Szafraniec J, Antosik A, Knapik-Kowalczuk J, et al. Molecular disorder of bicalutamide—amorphous solid dispersions obtained by solvent methods. *Pharmaceutics* 2018; 10: 194.
34. Tayyab Ansari M, Arshad MS, Hussain A, et al. Improvement of solubility, dissolution and stability profile of artemether solid dispersions and self emulsified solid dispersions by solvent evaporation method. *Pharm Dev Technol* 2018; 23: 1007-1015. 2016/11/26. DOI: 10.1080/10837450.2016.1265554.
35. Hadi AS and Ghareeb MM. Rizatriptan benzoate nanoemulsion for intranasal drug delivery: preparation and characterization. *International Journal of Drug Delivery Technology* 2022; 12: 546-552.
36. Omar TN, Mahdi MF, Al-Mudhafar MMJ, et al. Synthesize of New Ibuprofen and Naproxen Sulphonamide Conjugate with Anti-Inflammatory Study and Molecular Docking Study. *International Journal of Pharmaceutical Quality Assurance* 2018; 9: 102-108.
37. Newa M, Bhandari KH, Li DX, et al. Preparation, characterization and in vivo evaluation of ibuprofen binary solid dispersions with poloxamer 188. *Int J Pharm* 2007; 343: 228-237. 2007/06/29. DOI: 10.1016/j.ijpharm.2007.05.031.
38. Chokshi RJ, Zia H, Sandhu HK, et al. Improving the dissolution rate of poorly water soluble drug by solid dispersion and solid solution: pros and cons. *Drug Deliv* 2007; 14: 33-45. 2006/11/17. DOI: 10.1080/10717540600640278.
39. Sharma A and Jain CP. Preparation and characterization of solid dispersions of carvedilol with PVP K30. *Res Pharm Sci* 2010; 5: 49-56. 2010/01/01.
40. Kadhim ZJ and Rajab NA. Formulation and characterization of glibenclamide nanoparticles as an oral film. *International Journal of Drug Delivery Technology* 2022; 12: 387-394.
41. Chen ML, Lesko L and Williams RL. Measures of exposure versus measures of rate and extent of absorption. *Clin Pharmacokinet* 2001; 40: 565-572. 2001/08/29. DOI: 10.2165/00003088-200140080-00001.
42. Zhao L, Shi X and Zhang J. The Simulation of the relevance of absorption rate constant and elimination rate constant to the plasma drug concentration. In: *2012 International Conference on Computer Science and Electronics Engineering* 2012, pp.420-424. IEEE.

43. Rathod S, Desai H, Patil R, et al. Non-ionic surfactants as a P-glycoprotein (P-gp) efflux inhibitor for optimal drug delivery—a concise outlook. *Aaps Pharmscitech* 2022; 23: 55.
44. Lespine A, Martin S, Dupuy J, et al. Interaction of macrocyclic lactones with P-glycoprotein: structure-affinity relationship. *Eur J Pharm Sci* 2007; 30: 84-94. 2006/12/01. DOI: 10.1016/j.ejps.2006.10.004.
45. Li Y, Li J, Zhang X, et al. Non-ionic surfactants as novel intranasal absorption enhancers: in vitro and in vivo characterization. *Drug delivery* 2016; 23: 2272-2279.
46. Qin X, Yuan F, Zhou D, et al. Oral characteristics of bergenin and the effect of absorption enhancers in situ, in vitro and in vivo. *Arzneimittelforschung* 2010; 60: 198-204. 2010/05/22. DOI: 10.1055/s-0031-1296273.